WE03A-2

A Q-band SiGe-HBT Cryogenic Colpitts VCO for Frequency-Division Multiplexed Quantum Computing

E. Vardarli[1], X. Jin[1], A. Y.-K. Chen[2], K. Aufinger[3], and M. Schröter[1]

[1]Chair for Electron Devices and Integrated Circuits, Dresden, Germany
[2]Department of Electrical and Computer Engineering, University of California, Santa Cruz, USA
[3]Infineon Technologies AG, Neubiberg, Germany

Outline

- Motivation
- Cryogenic Device Characteristics
  - Transfer Characteristics / Transit Frequency / Noise Figure
- Circuit Description and Design
- Measurement Setup
- Measurement Results
  - Tuning Range / Output Power / Phase Noise /Spectrum
- Performance Summary
- Conclusion

Motivation (I)

- Fault-tolerant quantum computers need thousands of qubits
- Highly energy-efficient control/read-out needed due to limited cooling power
- Frequency-division multiplexing (FDM) enables simultaneous control/ read-out of qubits
  - Reduces number of LO generators
  - Reduces interface complexity between quantum processor and control/read-out electronics

Motivation (II)

- FDM requires increased IF bandwidth to allow multiple channels
  - Moving to millimeter-wave frequency bands (> 30 GHz)
    - Higher channel spacing (guard band) to avoid complex/power hungry pulse shaping
    - Area reduction of LC matching for gate-based read-out of spin qubits (on-chip)

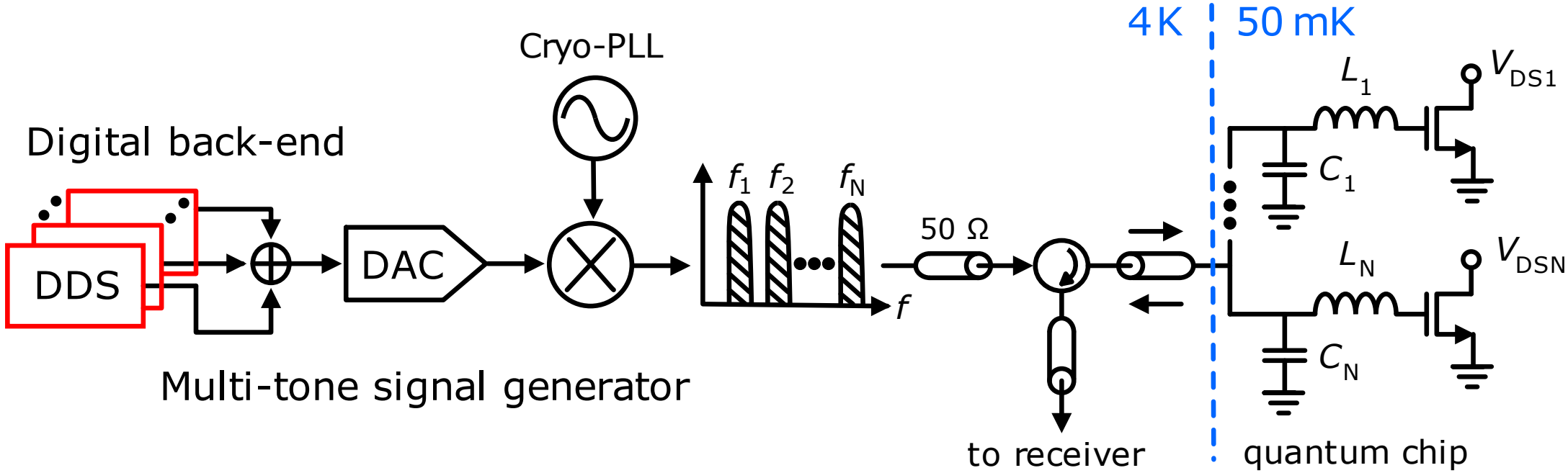

Cryogenic Device Characteristics

HICUM/L2 model

Cryogenic model extensions

→ tunneling currents*

→ parasitic resistances (R_{Cx} ,R_{Bx} ,R_E)

Parameter extraction of devices at 4K

→ DC and S-parameter measurement

→ 0.13 µm SiGe-HBT BiCMOS (Infineon AG)

→ CBEBC and BEC configuration

→ l_E = 1 µm to 10 µm

* M. Schröter and X. Jin, "A physics-based analytical formulation for the tunneling current through the base of bipolar transistors operating at cryogenic temperatures," *IEEE Trans. Electron Devices*, vol. 70, no. 1, pp. 247–253, Jan. 2023.

Cryogenic Device Characteristics (Transfer Characteristics)

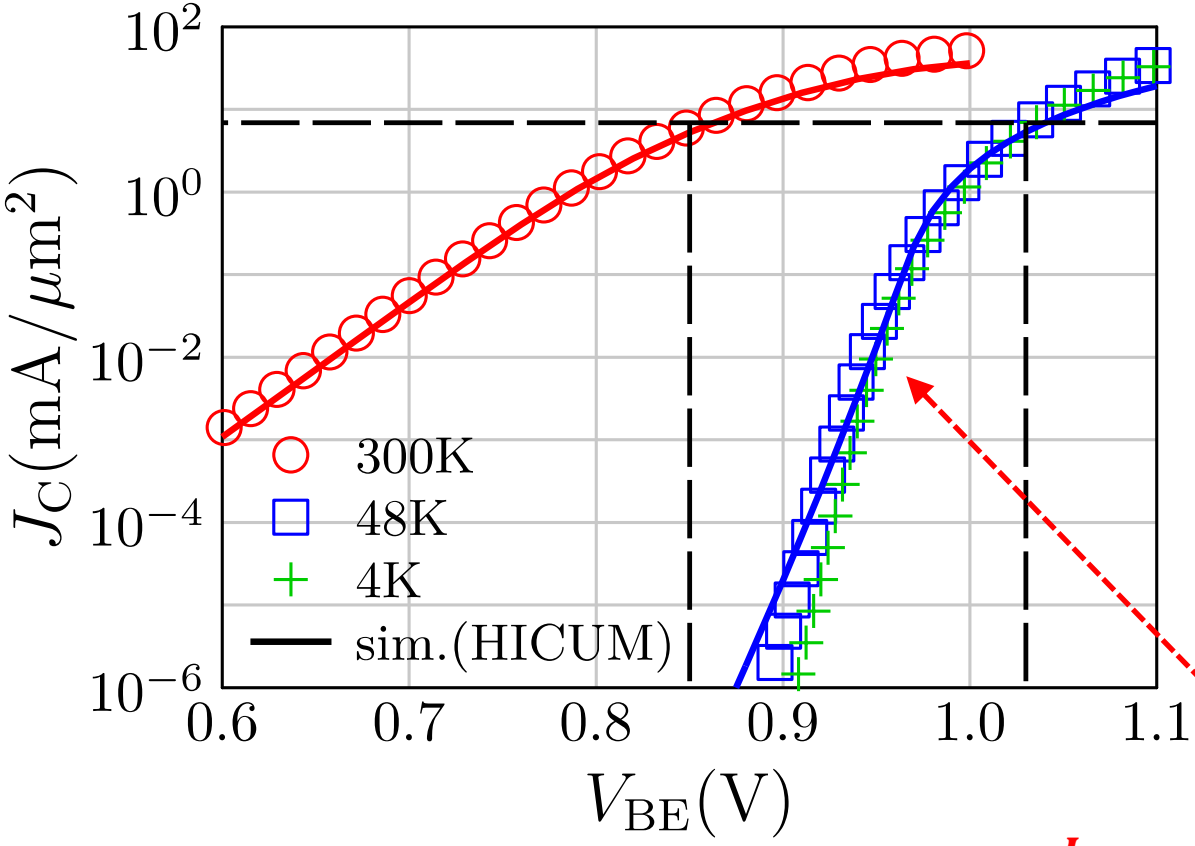

- Built-in voltage increases by 160 mV
  - V_{BE} increased for the same current density
- No improvement/change after 48 K
  - Model parameters are optimized at 48 K
  - Facilitate transient simulation convergence

✓ $g_m = \frac{I_C}{V_T}$ is improved greatly at low/medium injection regime

Cryogenic Device Characteristics (Transit Frequency)

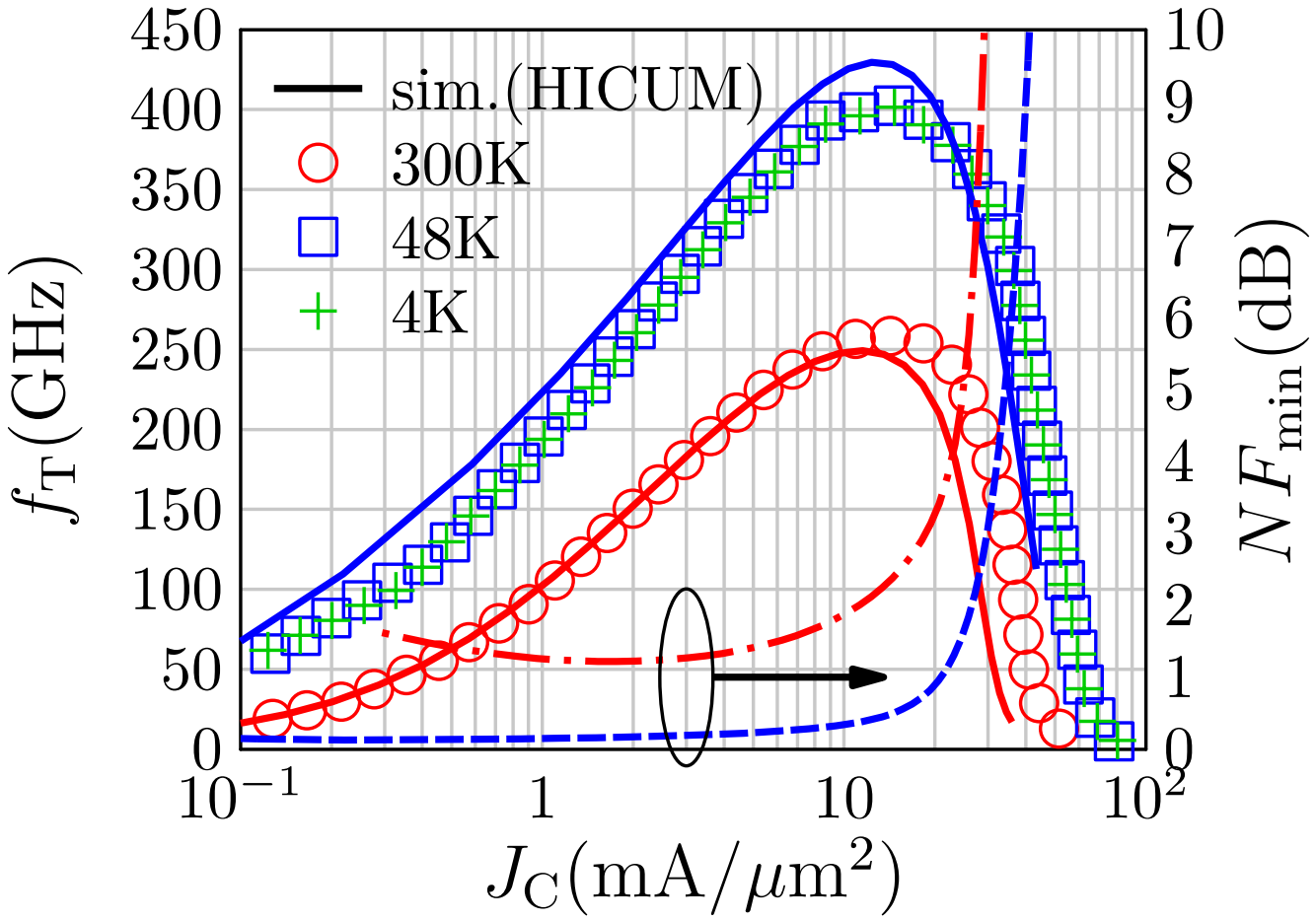

Peak transit frequency improves by a factor of 1.6

- No improvement after **48 K**
- Increase in g_m
- Decrease in R_{Cx} ,R_{Bx} ,R_E

Cryogenic Device Characteristics (Noise Figure at Q-band)

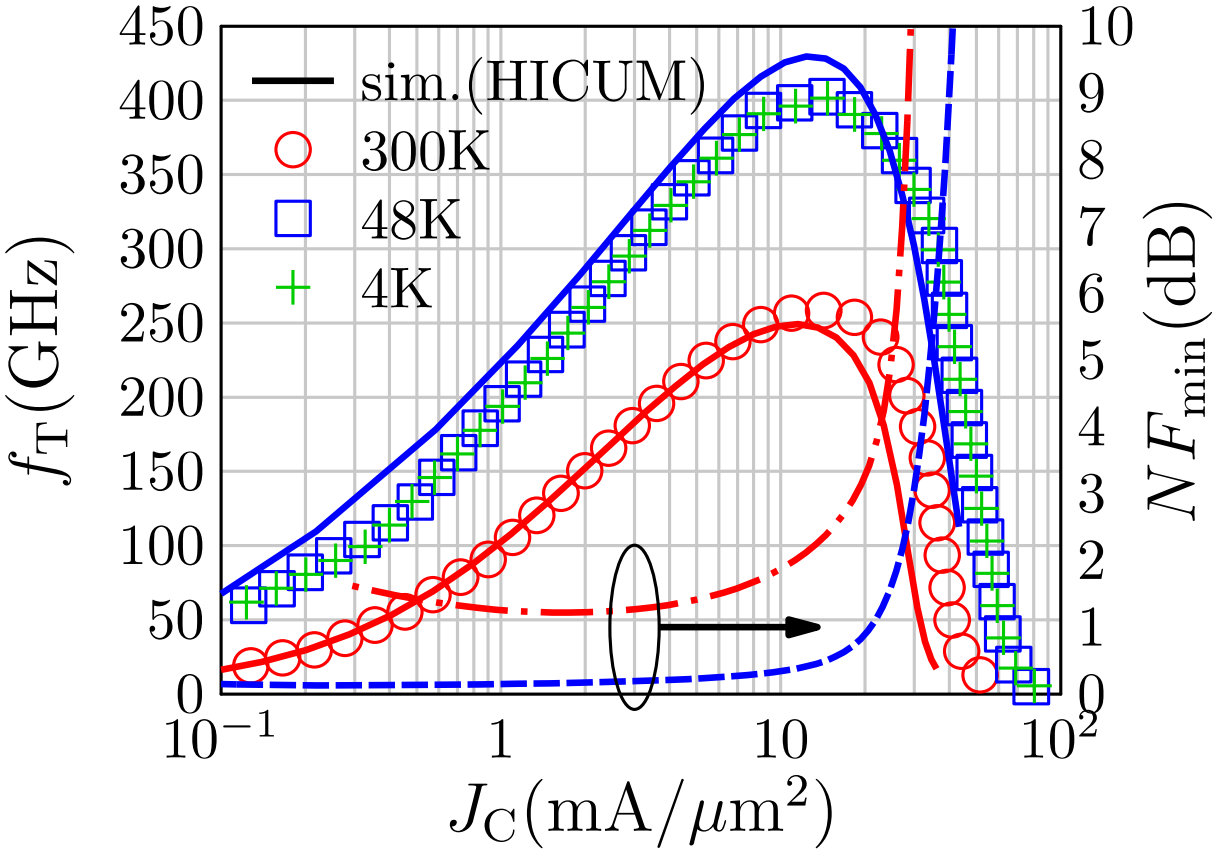

- NF_{min} drops much below 1 dB at 4K
  - Due to thermal noise sources (4kT↓ R↓)
    → R_{Bi0}, R_{Bx}, R_{Cx}, R_E
  - Noise temperature is used instead as metric

$$T_{MIN} = T_0 \cdot (10^{(NF_{MIN}/10)} - 1)$$

- Bias below 10 mA/μm^2 for lower shot noise
- Device noise increases phase noise†

† E. Vardarli *et al.*, "A W-band SiGe-HBT Colpitts VCO for millimeter-wave applications with an analog tuning range of 12%," *22nd Top. Meeting Silicon Monolithic Integr. Circuits RF Syst. (SiRF),* Las Vegas, NV, USA, Jan. 2022, pp. 81–84.

Circuit Description and Design

- Differential common-collector Colpitts topology
  - Oscillation determined by L_B and C_{varac}
  - The cascode buffer enables current re-use and isolation
  - Active current source used to adjust current densities
  - 18 mA DC current targeted for high output power
- Unsalicided polysilicon resistors used for biasing
  - Lowest temperature dependence (5 %)
  - Unit cells are used in resistive dividers to cancel temperature dependence on geometry

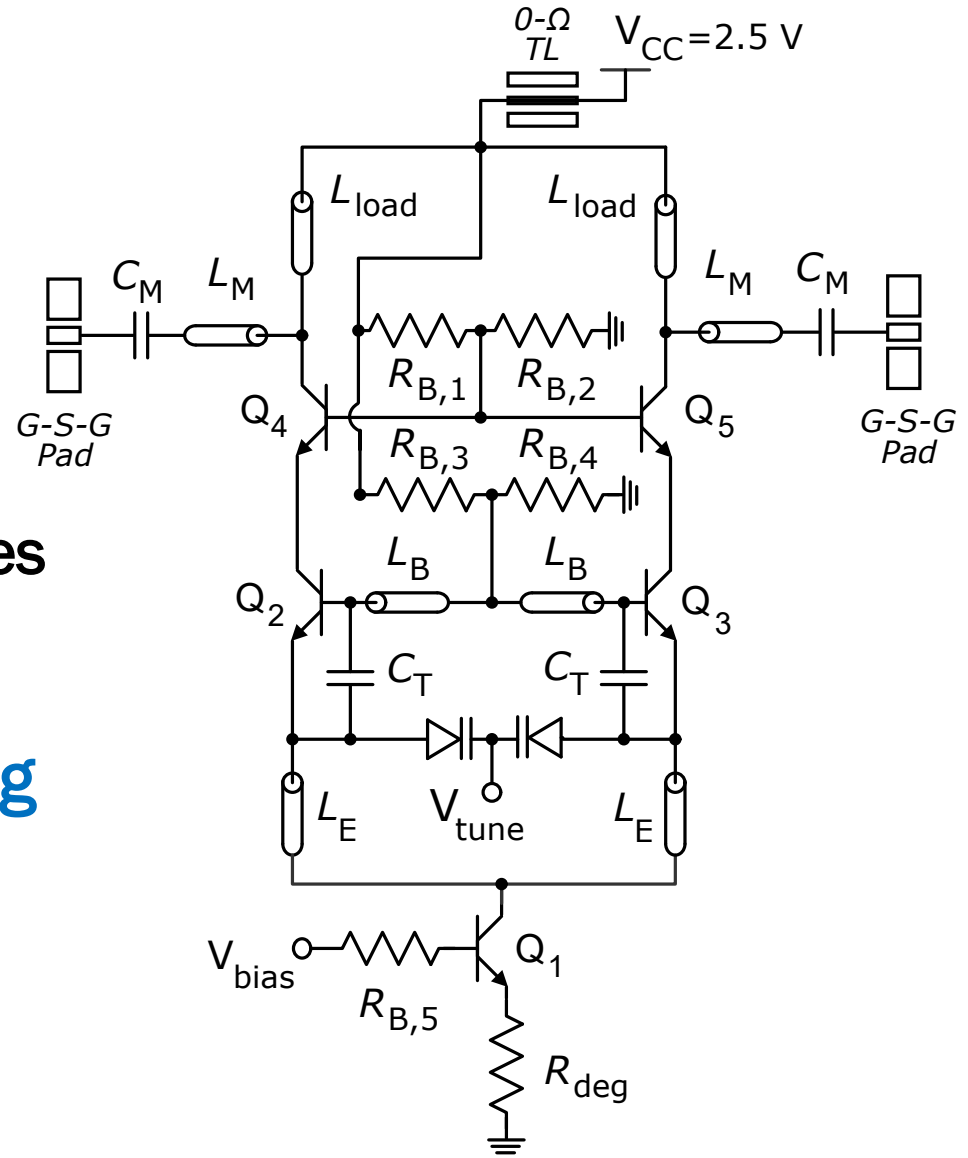

Circuit Description and Design

- Phase noise determined by :

$$L(\Delta\omega) = 10 \cdot \log\left(2 \cdot \frac{\overline{|I_n|^2}}{|V_{tank}|^2 (C_T + C_{BE})^2} \cdot \frac{C_{var}}{(C_T + C_{BE} + C_{var})\Delta\omega^2}\right)$$

- To improve phase noise :

– maximize the sum $(C_T + C_{BE})$ and chose $(C_T + C_{BE}) \gg C_{var}$

– ↑ V_{tank} (tank voltage swing) → low bound on J_C

– ↓ I_n (noise current spectral density) → high bound on J_C

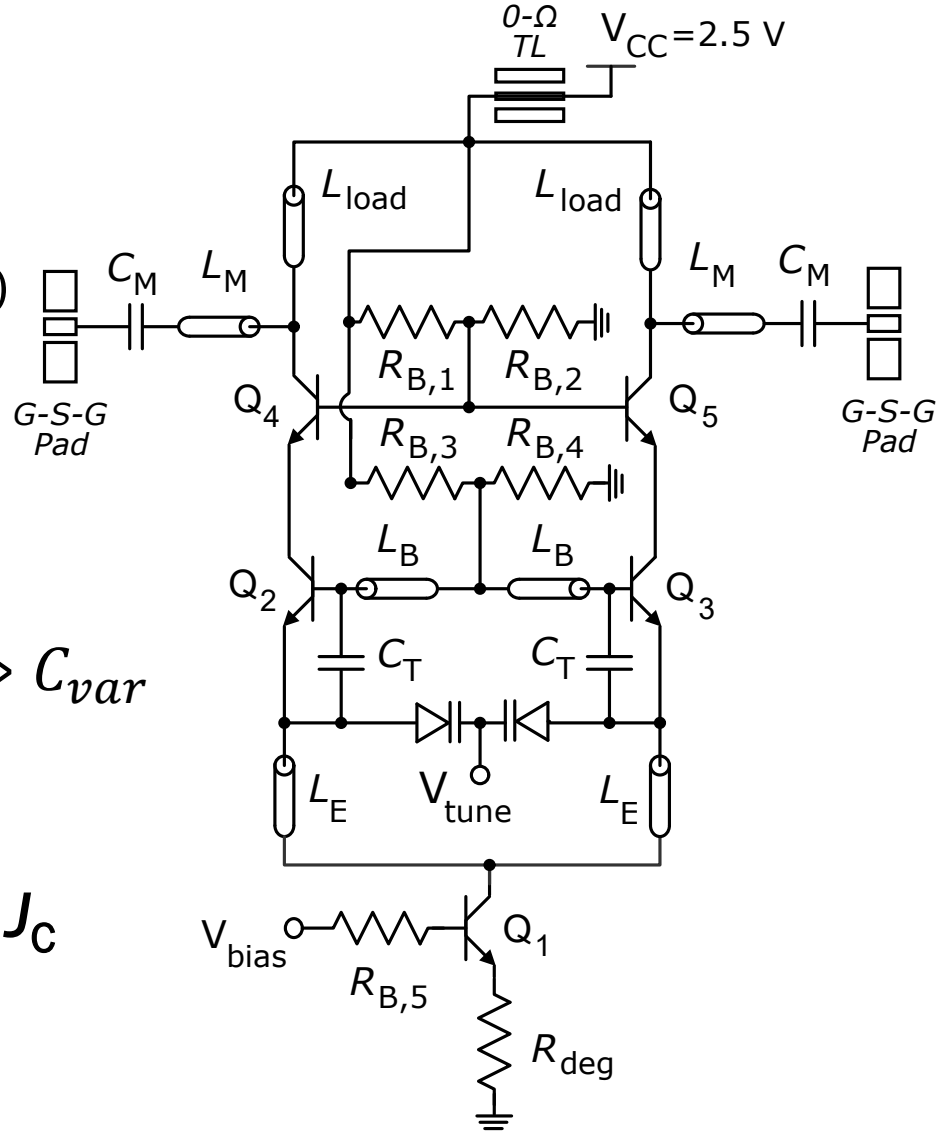

Measurement Setup

LakeShore Cryotronics table-top probe station (TTPX)

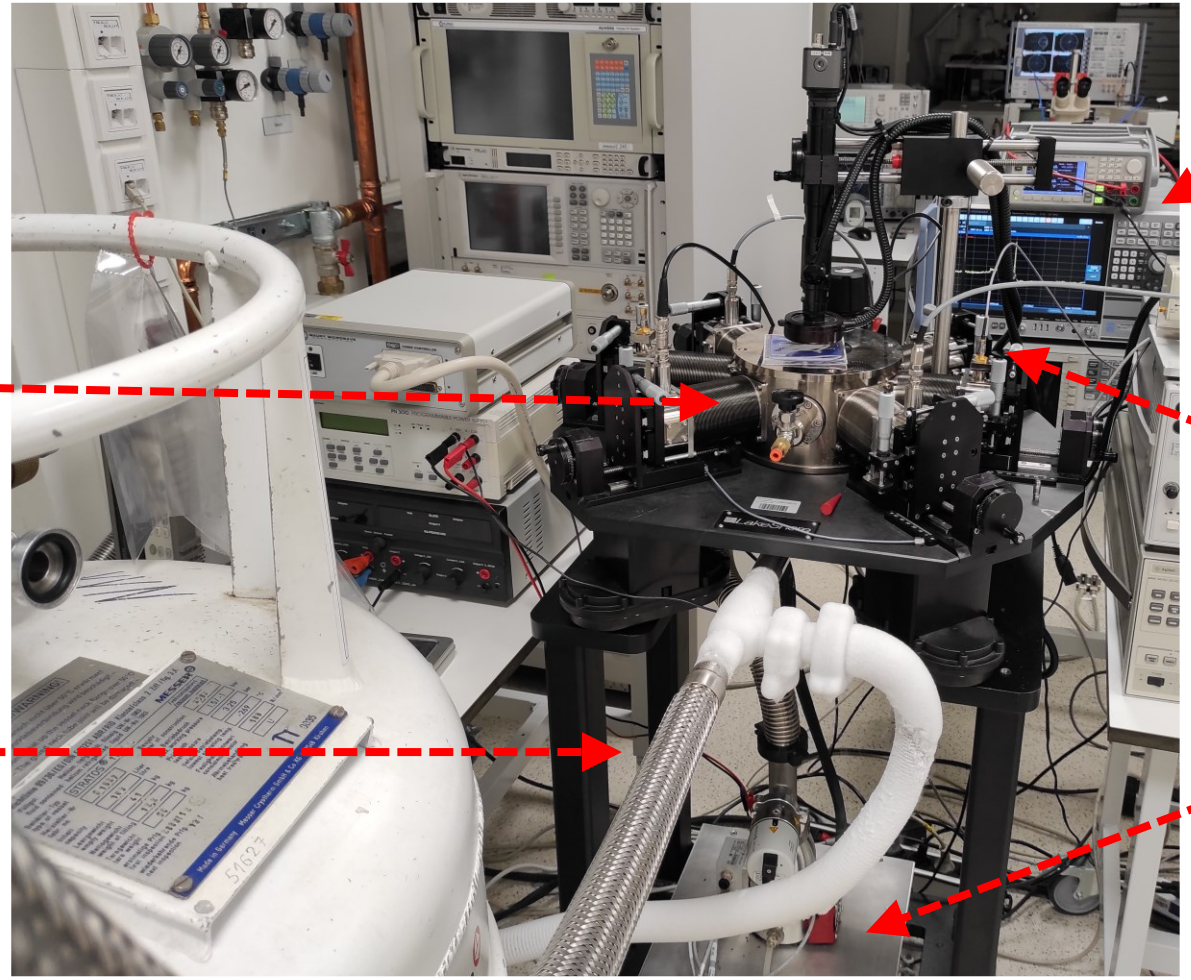

Six probe arms in total (four DC needles, two RF probes)

Liquid helium fed to the chamber through transfer line

FSW67 spectrum analyzer, DC supply

Insertion loss of cables and probes measured with PNA-X

Vacuum pump lowers the air pressure to 10^{-6} bar

Measurement Setup (layout)

- Cryogenic GSG probes (67 GHz) are used
- OUT- is terminated with an off-chip 50-Ω load
- Only a single ground pad is probed due to limitation
- 0-Ω line provides wideband AC grounding
- Area is 820 µm x 540 µm including pads
- All components EM-simulated with ADS momentum

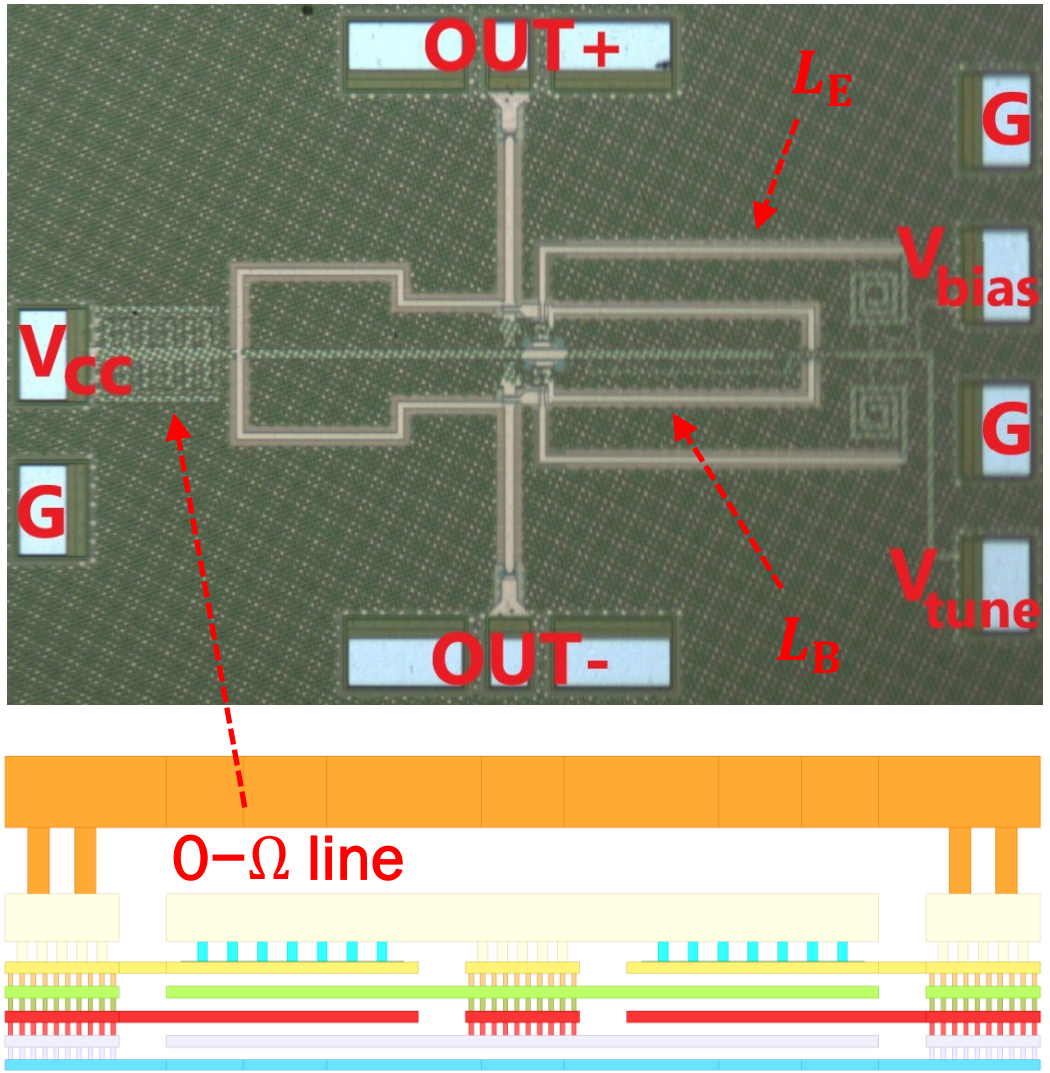

Measured Tuning Range

- 13 % fractional bandwidth at RT (39.5 to 45 GHz)
- Tuning range drops at 4 K due to earlier varactor saturation
  - Leads to degradation of C_{max}/C_{min}
- Higher oscillation frequency
  - Depletion capacitances decrease at CT
    - Higher junction built-in voltage
  - Diode-varactor capacitance can be fitted
    - C_{j0} (15 % ↓), V_{bi} (200 mV ↑), m ($\frac{C_{max}}{C_{min}}$ ↓)
- Tuning range improvement
  - Weakly dependent MOM capacitor array

$$C_j = \frac{C_{j0}}{(1 - \frac{V_{pn}}{V_{bi}})^m}$$

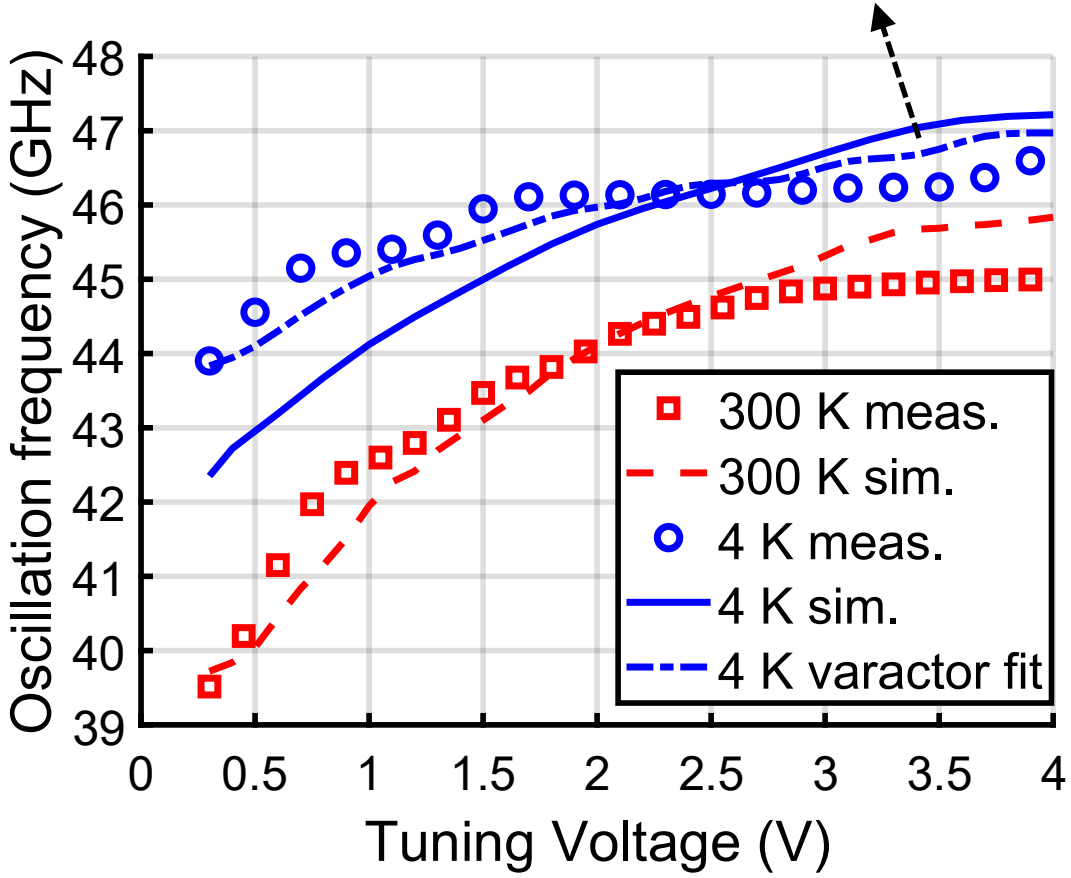

Measured Output Power

- 5.8 dBm single-ended output power at CT
  - Variation of only 0.8 dB across tuning range
  - High DC current needed to reach this level
- Improvement compared to RT due to :
  - Higher Q-factor of passive elements
    - higher metal conductivity
    - lower substrate loss due to higher resistivity
  - Increased g_m
- Two outputs enable PLL integration
  - High power relaxes LO buffer requirements for I/Q mixers
  - 2nd output can drive a divider chain with high isolation

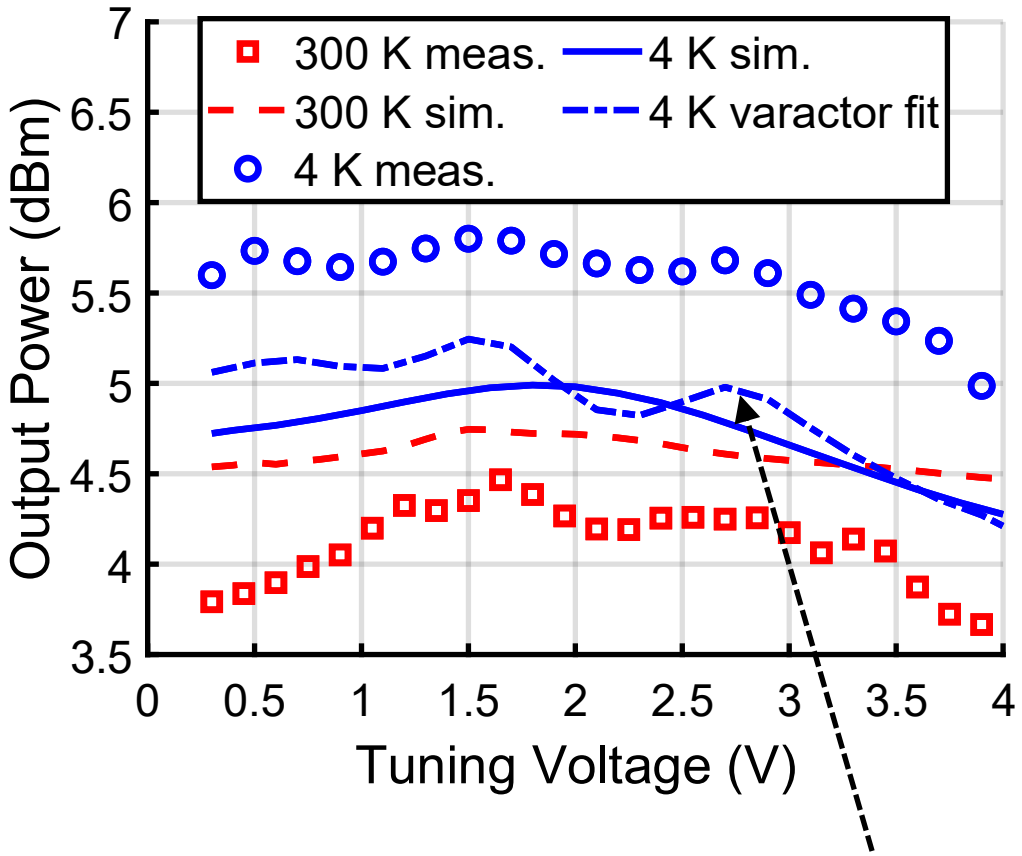

Profile is accurately captured with varactor fitting

Measured Phase Noise

- Improvement in phase noise is observed at 4K
  - Q-factor of the tank is higher
    - Freeze-out of low-doped substrate
    - Varactor Q-factor expected to improve
  - Thermal noise of devices/resistors is lower
    - Lower noise floor (N=kTB)
    - Lower phase noise at -20 dB/dec region

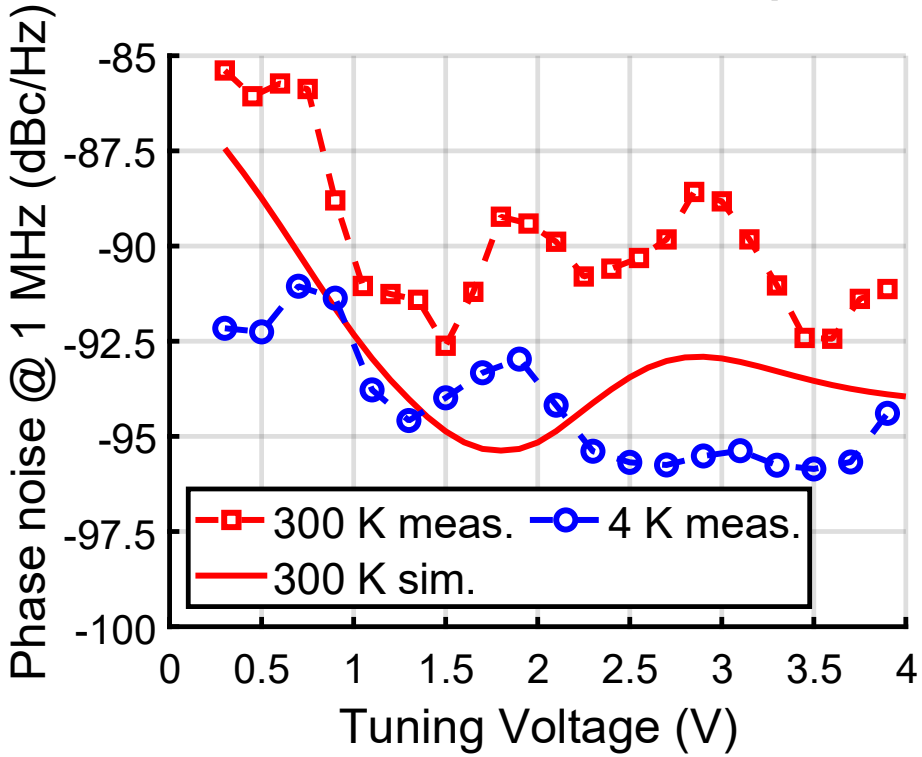

- Less improvement @ 1 MHz offset
- Higher $1/f^3$ PN corner at CT

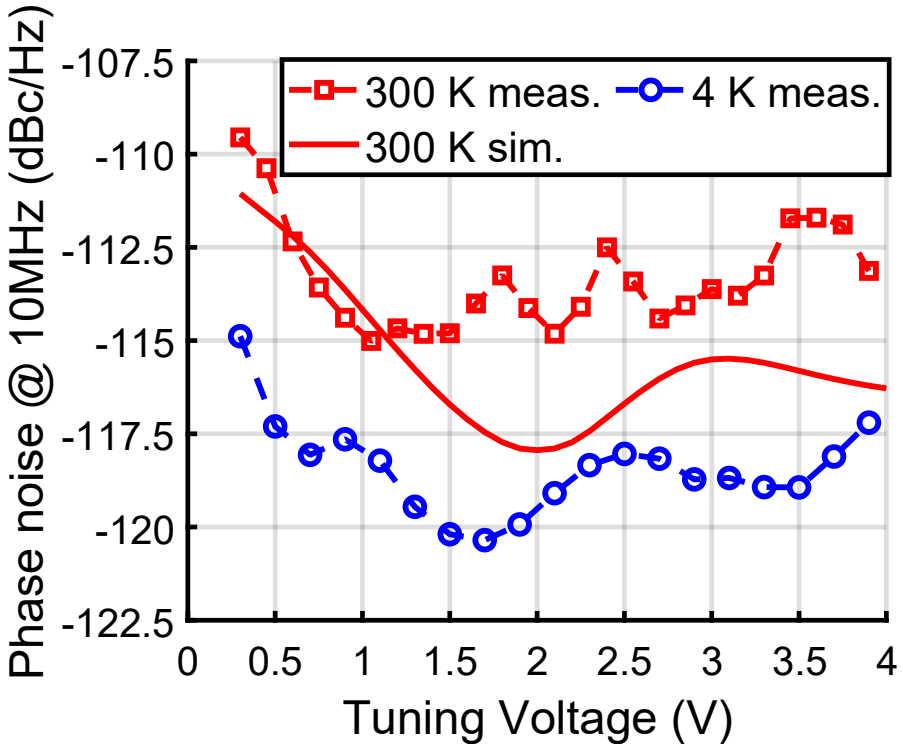

Measured Spectrum @ 4K

→ Clean spectrum is observed at Q-band

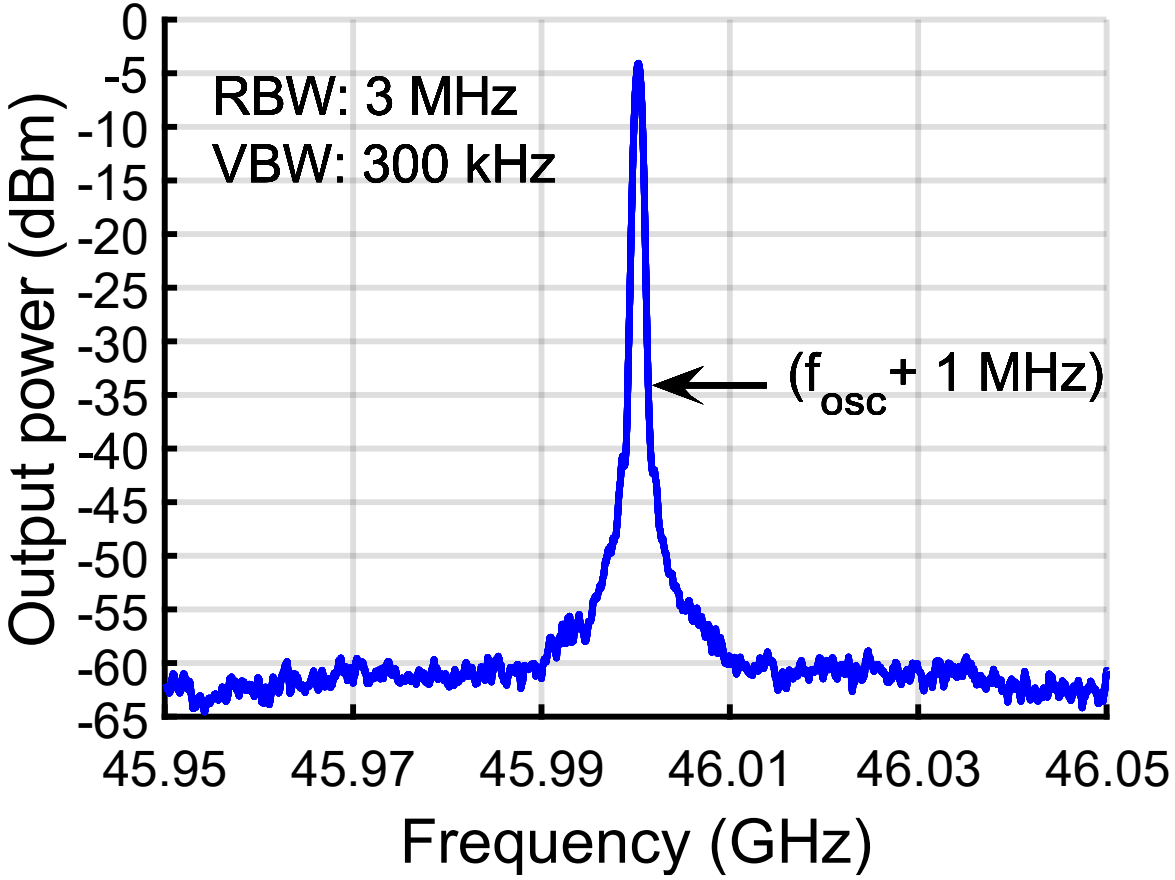

→ Flicker phase noise corner is at 1.3 MHz

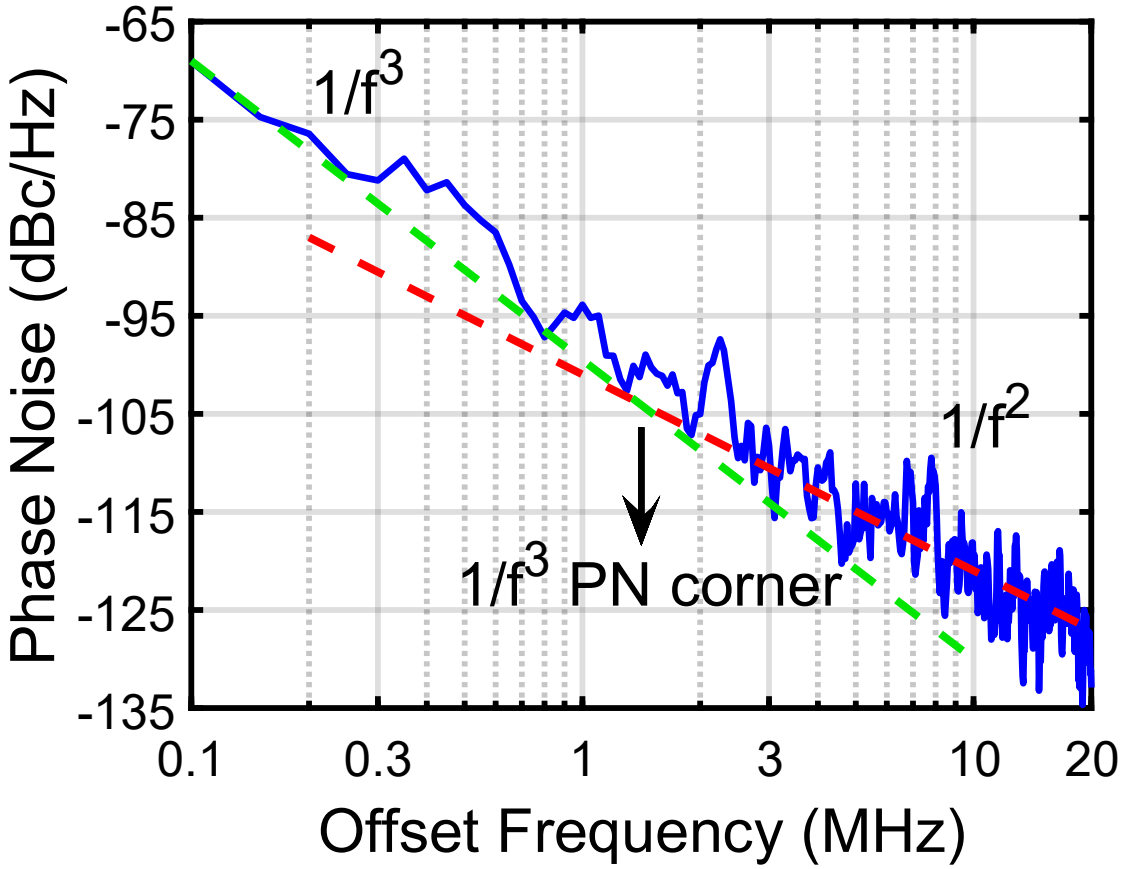

Performance Summary

	ISSCC 2022 [11]	ISSCC 2021 [7]	CICC 2021 [9]	RSI 2018 [17]	This Work
Technology	130 nm SiGe	40 nm CMOS	40 nm CMOS	130 nm SiGe	130 nm SiGe
Temperature (K)	3.5	4.2	4.2	4	4
Frequency (GHz)	15.9	12.7	10.8	33.7	45.2
Tuning Range	13.9-18.1	N/A	9.4-11.6	30.7-36.7	43.9-46.5
P_{DC} (mW)	3.1	4.4	1.7	112	45
P_{OUT} (dBm)	N/A	N/A	N/A	´-21.5	5.8
PN @ 1MHz / 10MHz (dBc/Hz)	-119.9 / -141.7	-114.5 / -136.2	-113 / -138	-110 / N/A	-95.8 / -120.3

- **Highest oscillation frequency**
- **Highest output power**
- **Coarse tuning can increase IF bandwidth → lower mW/qubit**

Conclusion

- Mm-wave cryogenic VCO with highest frequency and output power
  - LO buffer requirement relaxed to drive I/Q mixer of read-out/control
- Model parameters of HICUM/L2 is extracted at CT
  - Reasonable agreement between measurement and simulation
  - Varactor and substrate modelling can lead to further improvement
- ~5 dB improvement in phase noise at 10 MHz offset
- Mm-wave operation allows high degree of multiplexing
  - Reduces mW/qubit and interconnect complexity

Back-up Slide

Bias Point Sweep

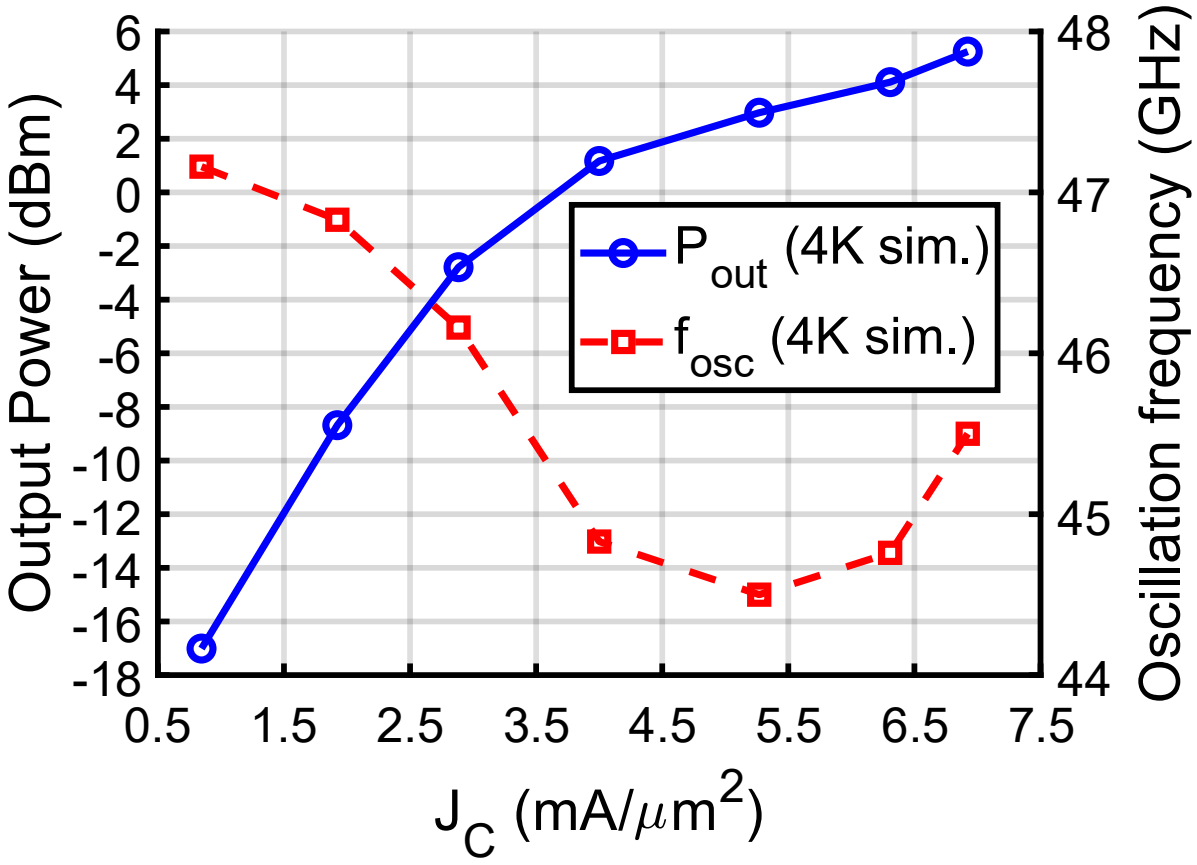

- Oscillator works down to 0.85 mA/μm^2 (5.5 mW power consumption)
- Lower output power
- Lower phase noise expected (harmonic balance convergence issue)